



Published in final edited form as:

Science. 2016 March 25; 351(6280): 1463–1469. doi:10.1126/science.aaf1490.

Clonal neoantigens elicit T cell immunoreactivity and sensitivity to immune checkpoint blockade

Nicholas McGranahan^{1,2,3,*}, Andrew J. S. Furness^{3,4,*}, Rachel Rosenthal^{3,*}, Sofie Ramskov⁵, Rikke Lyngaa⁵, Sunil Kumar Saini⁵, Mariam Jamal-Hanjani³, Gareth A. Wilson^{1,3}, Nicolai J. Birkbak^{1,3}, Crispin T. Hiley^{1,3}, Thomas B. K. Watkins^{1,3}, Seema Shafi³, Nirupa Murugaesu³, Richard Mitter¹, Ayse U. Akarca^{4,6}, Joseph Linares^{4,6}, Teresa Marafioti^{4,6}, Jake Y. Henry^{3,4}, Eliezer M. Van Allen^{7,8,9}, Diana Miao^{7,8}, Bastian Schilling^{10,11}, Dirk Schadendorf^{10,11}, Levi A. Garraway^{7,8,9}, Vladimir Makarov¹², Naiyer A. Rizvi¹³, Alexandra Snyder^{14,15}, Matthew D. Hellmann^{14,15}, Taha Merghoub^{14,16}, Jedd D. Wolchok^{14,15,16}, Sachet A. Shukla^{7,8}, Catherine J. Wu^{7,8,17,18}, Karl S. Peggs^{3,4}, Timothy A. Chan¹², Sine R. Hadrup⁵, Sergio A. Quezada^{3,4,†}, and Charles Swanton^{1,3,†}

¹The Francis Crick Institute, London WC2A 3LY, UK

²Centre for Mathematics and Physics in the Life Sciences and Experimental Biology (CoMPLEX), University College London (UCL), London WC1E 6BT, UK

³Cancer Research UK Lung Cancer Centre of Excellence, UCL Cancer Institute, London WC1E 6BT, UK

⁴Cancer Immunology Unit, UCL Cancer Institute, UCL, London WC1E 6BT, UK

⁵Section for Immunology and Vaccinology, National Veterinary Institute, Technical University of Denmark, 1970 Frederiksberg C, Denmark

⁶Department of Cellular Pathology, UCL, London WC1E 6BT, UK

⁷Department of Medical Oncology, Dana-Farber Cancer Institute, Boston, MA 02215, USA

⁸Broad Institute of MIT and Harvard, Cambridge, MA 02142, USA

⁹Center for Cancer Precision Medicine, Dana-Farber Cancer Institute, Boston, MA 02215, USA

¹⁰Department of Dermatology, University Hospital, University Duisburg–Essen, 45147 Essen, Germany

¹¹German Cancer Consortium (DKTK), 69121 Heidelberg, Germany

¹²Human Oncology and Pathogenesis Program, Memorial Sloan Kettering Cancer Center, New York, NY 10065, USA

[†]Corresponding author. E-mail: s.quezada@ucl.ac.uk (S.A.Q.); charles.swanton@crick.ac.uk (C.S.).

*These authors contributed equally to this work.

SUPPLEMENTARY MATERIALS

www.sciencemag.org/content/351/6280/1463/suppl/DC1

Materials and Methods

Figs. S1 to S7

Tables S1 to S5

References (22–38)

¹³Hematology/Oncology Division, 177 Fort Washington Avenue, Columbia University, New York, NY 10032, USA

¹⁴Department of Medicine, Memorial Sloan Kettering Cancer Center, New York, NY 10065, USA

¹⁵Weill Cornell Medical College, New York, NY 10065, USA

¹⁶Ludwig Collaborative Laboratory, Memorial Sloan Kettering Cancer Center, New York, NY 10065, USA

¹⁷Department of Medicine, Harvard Medical School, Boston, MA 02115, USA

¹⁸Department of Internal Medicine, Brigham and Woman's Hospital, Boston, MA 02115, USA

Abstract

As tumors grow, they acquire mutations, some of which create neoantigens that influence the response of patients to immune checkpoint inhibitors. We explored the impact of neoantigen intratumor heterogeneity (ITH) on antitumor immunity. Through integrated analysis of ITH and neoantigen burden, we demonstrate a relationship between clonal neoantigen burden and overall survival in primary lung adenocarcinomas. CD8⁺ tumor-infiltrating lymphocytes reactive to clonal neoantigens were identified in early-stage non-small cell lung cancer and expressed high levels of PD-1. Sensitivity to PD-1 and CTLA-4 blockade in patients with advanced NSCLC and melanoma was enhanced in tumors enriched for clonal neoantigens. T cells recognizing clonal neoantigens were detectable in patients with durable clinical benefit. Cytotoxic chemotherapy-induced subclonal neoantigens, contributing to an increased mutational load, were enriched in certain poor responders. These data suggest that neoantigen heterogeneity may influence immune surveillance and support therapeutic developments targeting clonal neoantigens.

Recent studies have highlighted the relevance of tumor neoantigens in the recognition of cancer cells by the immune system (1–4), prompting a renewed interest in personalized vaccines and cell therapies that target cancer mutations (5, 6). However, although genomic data are revealing the extent of genetic heterogeneity within single tumors (7), the influence of intratumor heterogeneity (ITH) upon the neoantigen landscape and sensitivity to immune modulation is unclear.

To explore neoantigen heterogeneity and its influence on antitumor immunity in early-stage non-small cell lung cancer (NSCLC), we applied a bioinformatics pipeline to seven primary NSCLCs subjected to multiregion sequence analysis (table S1) (8, 9). In total, 2860 putative neoantigens were predicted across the cohort, with a median of 326 neoantigens predicted per tumor (range of 80 to 741) (Fig. 1A). Neoantigen heterogeneity varied considerably, with an average of 44% neoantigens found heterogeneously, in a subset of tumor regions (range of 10 to 78%).

To address the clinical relevance of neoantigen burden and, specifically, the importance of clonal (present in all tumor cells) versus subclonal (present only in a subset) neoantigens, we subjected a predominantly early-stage cohort of 106 stage I/II, 43 stage III/IV, and 1 unknown-stage lung adenocarcinoma (LUAD) and 92 stage I/II and 32 stage III/IV lung squamous cell carcinoma (LUSC) cases from The Cancer Genome Atlas (TCGA) to

neoantigen and clonality analysis (10–12) (Fig. 1B). In this setting, to determine clonality from sequencing of a single sample, the cancer cell fraction, which describes the proportion of cancer cells harboring a mutation, was determined for each neoantigen (13).

A high neoantigen burden, defined as the upper quartile of neoantigen load, was associated with significantly longer overall survival in LUAD ($P=0.025$) (Fig. 1, C and D, and fig. S1A), and a trend for homogeneous tumors (neoantigen ITH $\geq 1\%$) to have longer overall survival times as compared with that of heterogeneous tumors was also observed ($P=0.061$) (fig. S1B). Although tumors with a high burden of neoantigens were found to be significantly more homogeneous than those with a low burden of neoantigens ($P<0.0001$, Wilcoxon rank-sum test) (fig. S1C), a combination of neoantigen ITH and neoantigen burden (as outlined in the schematic in Fig. 1C) was more significant than simply considering either metric alone and was observed across multiple different neoantigen ITH thresholds (without ITH threshold, $P=0.025$; ITH threshold = 0, $P=0.019$; ITH threshold = 0.01, $P=0.0096$; ITH threshold = 0.05, $P=0.021$) (Fig. 1D), remaining significant in multivariate analysis when including the tumor stage (table S2).

Despite a comparable range of predicted neoantigens in LUSC, no statistically significant association between overall survival and neoantigen load was observed in this subtype, even when incorporating neoantigen ITH (fig. S2, A to D). To investigate the reason for this disparity, we explored whether any immune-regulatory genes were differentially expressed between these two cancer types. Human lymphocyte antigen (HLA) class I genes—including *HLA-A*, *HLA-B*, *HLA-C*, *HLA-E*, *HLA-F*, and *HLA-G*, as well as β_2 microglobulin (β_2M), a component of the major histocompatibility complex (MHC) class I molecule—were expressed at a significantly lower level in LUSC as compared with LUAD (fig. S3A and table S3A), and this difference was observed across all levels of neoantigen burden (fig. S3B and table S3B). HLA class I genes were also down-regulated compared with matched normal samples in LUSC (table S3C). These data suggest that the presence of a high number of clonal neoantigens in homogeneous LUAD may favor effective immune surveillance, whereas in LUSC, immune escape may be more prevalent through HLA down-regulation.

We next evaluated whether immune-related genes were differentially expressed between homogeneous LUAD tumors ($\geq 1\%$ neoantigen ITH) with a high clonal neoantigen burden (greater than or equal to upper-quartile clonal neoantigens) compared with heterogeneous ($>1\%$ neoantigen ITH) or low clonal neoantigen burden tumors (less than upper-quartile clonal neoantigens). Eight genes were found to be significantly differentially expressed between these two groups (table S4A). Programmed cell death ligand-1 (PD-L1) and the proinflammatory cytokine interleukin-6 (IL-6) were the most significantly differentially expressed genes, up-regulated in the homogeneous and high clonal neoantigen group. When we specifically compared tumors in the upper quartile of clonal neoantigen burden with tumors in the lower quartile, we identified an additional 25 significantly differentially expressed genes (table S4B and fig. S4A). CD8A, CD8B, and genes associated with antigen presentation (*TAP-1*, *TAP-2*, and *STAT-1*), T cell migration (*CXCL-10* and *CXCL-9*), and effector T cell function [interferon- γ (IFN- γ) and granzymes B, H, and A] were up-regulated in the high clonal neoantigen cohort and found to cluster together, indicating

coexpression (fig. S4B). PD-1 and lymphocyte activation gene 3 (LAG-3)—negative regulators of T cell function (14)—were also identified in this cluster, as were the ligands PD-L1 and PD-L2.

These data suggest that a high clonal neoantigen burden in LUAD is associated with an inflamed tumor microenvironment enriched with activated effector T cells, potentially regulated by inhibitory immune checkpoint molecules and their ligands. We therefore attempted to identify and characterize T cells reactive to neoantigens in patients with early-stage NSCLC. We focused on two tumors, L011 and L012, with a comparable number of predicted neoantigens and a similar smoking history, but divergent levels of neoantigen ITH (8 versus 74% heterogeneous predicted neoantigens) (Fig. 2, A to C). We used 288 and 354 putative neoantigen-loaded, HLA-matched multimers derived from L011 and L012, respectively, to screen CD8⁺ T cells expanded from individual tumor regions and adjacent normal lung tissue, using a previously described high-throughput method (Fig. 2, D and E) (15).

CD8⁺ T cells reactive to mutant MTFR2^{D326Y} (FAFQEYDSF) were identified in L011, whereas in L012, two distinct CD8⁺ T cell responses to mutant CHTF18^{L769V} (LLDIVAPK) and MYADM^{R30W} (SPMIVGSPW) were observed (Fig. 2, D and E, and fig. S5, A and B). MTFR2^{D326Y}, CHTF18^{L769V}, and MYADM^{R30W} all represent clonal neoantigens, suggesting that immune-reactivity against clonal neoantigens can be detected in both homogeneous and heterogeneous NSCLC. High HLA binding affinity was predicted for MTFR2^{D326Y} and CHTF18^{L769V} in both wild-type and mutant forms, but only the mutant peptide was found to elicit a T cell response. Higher binding affinity to mutant versus wild-type form was predicted for MYADM^{R30W}; however, in this case, reactivity toward wild-type peptide was also observed (fig. S5C). The mutation in the MYADM^{R30W} peptide lies in the anchor residue, primarily affecting HLA binding and not T cell recognition. Although the data suggest that T cells in this patient can recognize both mutant and wild-type peptides when stabilized within a MHC-multimer system, the very low predicted affinity of the wild-type peptide to HLA would be expected to prevent adequate presentation in vivo.

We next used MHC multimers that identify neoantigen-reactive T (NAR-T) cells to characterize NAR-T cells in unexpanded samples (Fig. 3, A to D). MTFR2^{D326Y}-reactive CD8⁺ T cells, identified in unexpanded L011, were analyzed by means of multicolor flow cytometry. We assessed relative expression of co-inhibitory immune checkpoint molecules and effector cytokines between tumor-infiltrating CD4⁺FoxP3⁺ (regulatory T cell), CD4⁺FoxP3⁻ (CD4⁺ helper T cell), CD8⁺ multimer negative, and CD8⁺ multimer-reactive (MTFR2^{D326Y}⁺) T cell subsets. MTFR2^{D326Y}⁺ CD8⁺ T cells expressed high levels of co-inhibitory receptors PD-1 and LAG-3 (Fig. 3C), which is consistent with our bioinformatics findings (fig. S4). Almost all NAR-T cells (97%) expressed high levels of PD-1, compared with 49% of multimer-negative tumor-infiltrating CD8⁺ T cells. CTLA-4 expression was largely confined to CD4⁺FoxP3⁺ regulatory T cells, which is consistent with preclinical findings (16). PD-1⁺ MTFR2^{D326Y}-reactive CD8⁺ T cells coexpressed high levels of granzyme B (GzmB) (74.8%) (Fig. 3D). Characterization of CHTF18^{L769V}- and MYADM^{R30W}-reactive CD8⁺ T cells mirrored findings in L011, with high expression of

PD-1 observed in 97% and 99.6% of CHFT18^{L769V}- and MYADM^{R30W}-reactive CD8⁺ T cells, respectively (fig. S5, D and E).

Given the potential ability of clonal neoantigens to promote priming and infiltration by neoantigen reactive T cells expressing high levels of PD-1, we explored whether response to PD-1 blockade in patients with advanced NSCLC may be influenced by neoantigen ITH. Exome sequencing data from a recent study in which 34 patients were treated with pembrolizumab— an antibody targeting PD-1—was obtained (table S5) (2), and the clonal architecture of each tumor estimated (possible for 31 of 34 tumors).

Neoantigen burden was related to clinical response to pembrolizumab, with a high neoantigen repertoire associated with improved outcome, as previously reported (Fig. 4A). However, consistent with the importance of clonal neoantigens, the clinical efficacy of PD-1 blockade also appeared related to the clonal architecture of each tumor (Fig. 4A), with tumors derived from patients with no durable benefit [defined as in (2)] exhibiting significantly higher neoantigen ITH than that of tumors from patients with a durable clinical benefit ($P=0.006$, Wilcoxon rank sum test). Almost every tumor (12 of 13) that exhibited a low neoantigen subclonal fraction (<5% subclonal) and high mutation burden (70, median clonal neoantigens of the cohort) demonstrated durable clinical benefit with anti-PD-1 therapy. Conversely, only 2 out of 18 tumors with a high subclonal neoantigen fraction (>5%) or low clonal neoantigen burden benefited from pembrolizumab (Y2087 and SB10944). For example, despite a large neoantigen burden, ZA6505 exhibited progressive disease, relapsing after 2 months. ZA6505 was one of the most heterogeneous tumors within the cohort, with over 80% of mutations classified as subclonal.

Tumors with both a high clonal neoantigen burden and low neoantigen ITH were associated with significantly longer progression-free survival, and this relationship remained robust to the choice of ITH threshold, with lower hazard ratios observed as compared with the use of neoantigen burden alone (Fig. 4B). The majority of clonal neoantigens could be attributed to smoking-induced mutations (Fig. 4A). Greater PD-L1 expression was observed in tumors harboring a large clonal neoantigen burden and low neoantigen heterogeneity compared with the remaining tumors ($P=0.0017$, χ^2 test) (Fig. 4A and fig. S6).

Next, we obtained data from 64 melanoma patients treated with either ipilimumab or tremelimumab, which are antibodies against CTLA-4 (4). Clonal architecture analysis was possible for 57 of 64 tumors, and significantly improved overall survival was observed in tumors exhibiting a low neoantigen ITH and a high clonal neoantigen burden. This relationship was observed when multiple different ITH thresholds were used, similar to the NSCLC cohort (ITH threshold = 0.01, $P=0.008$; ITH threshold = 0.02, $P=0.011$; ITH threshold = 0.05, $P=0.083$) (Fig. 4C). The relationship between neoantigen burden and survival outcome was not statistically significant without an ITH threshold ($P=0.083$) (Fig. 4C).

To address whether radiation or cytotoxic exposure might stimulate production of subclonal neoantigens that could contribute to total neoantigen burden but not the efficacy of checkpoint blockade, sequencing data from a more heavily pretreated melanoma cohort,

comprising 110 tumors, were obtained (17). For the subset of tumors for which clonal analysis was possible (78 of 110 tumors, a smaller and less adequately powered cohort as compared with the published analysis), total neoantigen burden was not significantly associated with efficacy of immune checkpoint inhibition [classified as in (17)], although a trend was observed ($P=0.24$, Wilcoxon rank sum test) (fig. S7A). However, an enrichment for tumors exhibiting high neoantigen heterogeneity or low clonal neoantigen burden (both stratified according to the median of the cohort) reached borderline significance in patients with minimal or no benefit compared with patients exhibiting a clinical benefit ($P=0.06$, Fisher's exact test). Neoantigen burden was not found to be significantly associated with overall survival in this cohort (fig. S7B). Two of the most heterogeneous tumors (Pat58 and Pat151) with minimal or no benefit were among those treated with the alkylating agent dacarbazine (DTIC) before anti-CTLA therapy, and for both, >98% of subclonal mutations were attributable to mutational Signature 11, a signature associated with prior exposure to alkylating agents (18, 19). One patient with stable disease—Pat80, who was also treated with DTIC before anti-CTLA-4 therapy—also harbored an increase in Signature 11 and progressed by 6 months [classified as no durable benefit according to (2)]. These data suggest that therapy may induce subclonal mutations that fail to drive an efficient antitumor response, although further data are needed to confirm this observation.

Last, we reasoned that T cells recognizing clonal antigens should be detectable in patients deriving favorable responses to checkpoint blockade. Previous analysis of peripheral blood lymphocytes (PBLs) from CA9903, a LUAD patient with an exceptional response to pembrolizumab, identified a CD8⁺ T cell population in autologous PBLs, recognizing a predicted neoantigen resulting from a HERC1^{P3278S} mutation (ASNASSAAK) (2). Consistent with the relevance of clonal neoantigens, this mutation was found to be present in 100% of cancer cells within the sequenced tumor (Fig. 4D). Similarly, analysis of peripheral blood mononuclear cells (PBMCs) from the patients with CR9309 and CR0095—melanomas that responded to anti-CTLA-4 therapy, resulting in prolonged patient survival—identified CD8⁺ T cell populations, recognizing tumor-specific neoantigens (4). In both cases, the neoantigens linked to a T cell response were derived from clonal mutations, predicted to be present in 100% of cancer cells (Fig. 4, E and F).

Previous studies have reported that neoantigen burden influences sensitivity to immune checkpoint blockade in NSCLC and melanoma (2, 4, 17). However, the influence of ITH on this relationship has not been investigated. Our results, although limited by access to small and diverse patient cohorts and single-site biopsy data that likely overestimate the number of clonal mutations, suggest that clonal and subclonal neoantigens do not drive equally effective antitumor immunity. Indeed, using the described approach, despite screening more than 250 peptides against putative subclonal neoantigens, we were only able to detect T cells that recognize clonal neoantigens. Conceivably, higher-neoantigen ITH may result in lower antigen dosage as compared with homogeneous tumors with high clonal neoantigen burden, thus reducing the chances of identifying T cells reactive to subclonal neoantigens. Furthermore, in cases in which T cells reactive to subclonal neoantigens are generated, these will be unable to target all tumor cells, limiting overall tumor control.

The observation that certain anti-CTLA-4 refractory tumors were enriched for subclonal mutations caused by alkylating agents suggests that mutations induced by therapy may enhance total neoantigen burden but might not elicit an effective antitumor response, possibly because of the subclonal nature of the neoantigens that results from cytotoxic exposure. These results highlight the need to consider both the antitumor effects of alkylating agents as well as the potential risk of inducing subclonal mutations (19).

The identification of cytotoxic tumor-infiltrating T cells that recognize clonal mutations, shared by all tumor cells, might hold promise for adoptive therapy strategies to address the challenges of ITH (20). The extensive clonal mutational repertoire present in smoking-associated NSCLC (8, 21) could render this disease vulnerable to vaccination or T cell therapies targeting multiple clonal neoantigens, in combination with appropriate immune checkpoint modulation.

Acknowledgments

C.S. is a senior Cancer Research UK (CRUK) clinical research fellow and is funded by CRUK (TRACERx), the CRUK Lung Cancer Centre of Excellence, Stand Up 2 Cancer Laura Ziskin prize (SU2C), the Rosetrees Trust, NovoNordisk Foundation (ID 16584), the Prostate Cancer Foundation, the Breast Cancer Research Foundation, the European Research Council (THESEUS), and EU FP7 (PREDICT). S.A.Q is funded by a CRUK Career Development Fellowship, CRUK Biotherapeutic Programme Grant, World Wide Cancer Research, and a Cancer Research Institute Investigator Award. A.J.S.F receives support from the Sam Keen Foundation. R.R., N.M., N.J.B., and G.A.W. are funded by the TRACERx CRUK grant. T.B.K.W. is funded by the FP7-People-2013-ITN [grant (2013)607722 – PloidyNet]. C.T.H. is funded by the Rosetrees Trust. C.J.W. is a Scholar of the Leukemia and Lymphoma Society and acknowledges support from the Blavatnik Family Foundation, NIH/National Heart, Lung, and Blood Institute (grant 1R01CA155010-02) and NIH/National Cancer Institute (grants 1R01CA182461-01 and 1R01CA184922-01). S.S. is funded by the Cancer Research UK–UCL Centre, and M.J.H. is funded by a CRUK–UCL Centre Clinical Research Fellowship. A.A. is funded by the Cancer Research UK–UCL Centre Cancer Immuno-Therapy Accelerator Award. We thank N. Hacohen and S. Turajlic for helpful advice on the manuscript. This research is supported by the National Institute for Health Research, the University College London Hospitals Biomedical Research Centre, and the Cancer Research UK University College London Experimental Cancer Medicine Centre. Certain data were received under a material transfer agreement with Memorial Sloan Kettering Cancer Center. Data from multiregion sequenced NSCLC are available at the European Bioinformatics Institute (accession no. EGAS00001000809). Data from the Rizvi cohort (2) are available at the database of Genotypes and Phenotypes (dbGAP) (accession no. phs000980.v1.p1). Data from the Snyder cohort (4) are available at dbGAP (accession no. phs001041.v1.p1). Data from the Van Allen cohort (17) are available at dbGAP (accession no. phs000452.v2.p1). The results published here are in part based on data generated by a TCGA pilot project established by the National Cancer Institute and National Human Genome Research Institute. The data were retrieved through dbGAP authorization (accession no. phs000178.v9.p8). Information about TCGA and the investigators and institutions that constitute the TCGA research network can be found at <http://cancergenome.nih.gov>. C.S. is a paid advisor for Janssen, Boehringer Ingelheim, Ventana, Novartis, Roche, Sequenom, Natera, Grail, Apogen Biotechnologies, Epic Biosciences, and the Sarah Cannon Research Institute. D.S. is a paid advisor for Bristol-Myers Squibb, Roche, Novartis, Merck, and Amgen. B.S. is a paid advisor for Bristol-Myers Squibb. T.A.C. is a cofounder of and holds equity in Gritstone Oncology; is a paid advisor for Geneocea, OncoSpire, and Cancer Genetics; and receives funding from Bristol-Myers Squibb for research on the genomics of immune response. N.A.R. is a cofounder of and holds equity in Gritstone Oncology. E.M.V.A. is a paid advisor for Syapse, Roche Ventana, Takeda, and Third Rock Ventures. M.D.H. is a paid advisor for Bristol-Myers Squibb, Merck, Genentech, AstraZeneca, and Neon. J.D.W. is a paid advisor for Bristol-Myers Squibb.

L.A.G. is a paid scientific advisor for Novartis, Boehringer Ingelheim, Foundation Medicine, and Warp Drive Bio. C.S., N.M., R.R., S.A.Q., and K.S.P. are co-inventors on UK patent applications (1516047.6, 1601098.5, 1601098.5, and 1601099.3) filed by Cancer Research Technology relating to methods for identifying and targeting neoantigens, methods of predicting prognosis of cancer patients, and/or identifying cancer patients who will benefit from treatment that involves determining the number of neoantigens.

REFERENCES AND NOTES

1. Matsushita H, et al. *Nature*. 2012; 482:400–404. [PubMed: 22318521]

2. Rizvi NA, et al. *Science*. 2015; 348:124–128. [PubMed: 25765070]
3. Castle JC, et al. *Cancer Res*. 2012; 72:1081–1091. [PubMed: 22237626]
4. Snyder A, et al. *N Engl J Med*. 2014; 371:2189–2199. [PubMed: 25409260]
5. Robbins PF, et al. *Nat Med*. 2013; 19:747–752. [PubMed: 23644516]
6. Schumacher TN, Schreiber RD. *Science*. 2015; 348:69–74. [PubMed: 25838375]
7. Greaves M. *Cancer Discovery*. 2015; 5:806–820. [PubMed: 26193902]
8. de Bruin EC, et al. *Science*. 2014; 346:251–256. [PubMed: 25301630]
9. Jamal-Hanjani M, et al. *Ann Oncol*. 2016:mdw037.
10. Lawrence MS, et al. *Nature*. 2014; 505:495–501. [PubMed: 24390350]
11. Rooney MS, Shukla SA, Wu CJ, Getz G, Hacohen N. *Cell*. 2015; 160:48–61. [PubMed: 25594174]
12. Shukla SA, et al. *Nat Biotechnol*. 2015; 33:1152–1158. [PubMed: 26372948]
13. Materials and methods are available as supplementary materials on Science Online.
14. Nguyen LT, Ohashi PS. *Nat Rev Immunol*. 2015; 15:45–56. [PubMed: 25534622]
15. Hadrup SR, et al. *Nat Methods*. 2009; 6:520–526. [PubMed: 19543285]
16. Read S, Malmström V, Powrie F. *J Exp Med*. 2000; 192:295–302. [PubMed: 10899916]
17. Van Allen EM, et al. *Science*. 2015; 350:207–211. [PubMed: 26359337]
18. Alexandrov LB, et al. *Nature*. 2013; 500:415–421. [PubMed: 23945592]
19. Johnson BE, et al. *Science*. 2014; 343:189–193. [PubMed: 24336570]
20. Yap TA, Gerlinger M, Futreal PA, Pusztai L, Swanton C. *Sci Transl Med*. 2012; 4:127ps10.
21. Zhang J, et al. *Science*. 2014; 346:256–259. [PubMed: 25301631]

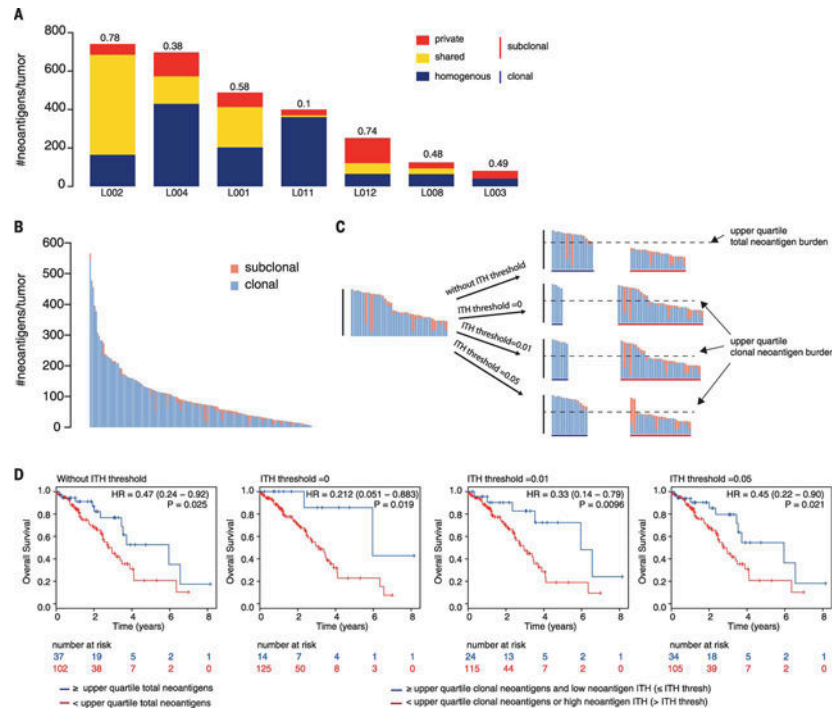


Fig. 1. Heterogeneity and prognostic value of neoantigen landscape in primary NSCLC
(A) Total putative neoantigen burden in multiregion sequenced NSCLC tumors. Proportion of clonal neoantigens, identified ubiquitously in every tumor region, are shown in blue; shared subclonal neoantigens, identified as shared in multiple tumor regions but not all, are shown in yellow; and private subclonal neoantigens, identified in only one tumor region, are in red. **(B)** Total putative neoantigen burden in TCGA LUAD tumors. Proportion of neoantigens arising from clonal (blue) or subclonal (red) mutations is shown. **(C)** Schematic illustrating use of different neoantigen ITH thresholds, with bar plot showing separation into the two groups. Without an ITH threshold, samples are simply grouped according to upper quartile of total neoantigen burden. For each ITH threshold, the upper quartile of clonal neoantigens is used to separate tumors with high and low clonal neoantigen burden, and the neoantigen ITH threshold further groups samples. For example, an ITH threshold = 0 involves grouping tumors with high clonal neoantigen burden and zero neoantigen heterogeneity separately from those with low clonal neoantigen burden or any neoantigen heterogeneity. **(D)** Overall survival curves for samples by using different ITH thresholds. Shown are without an ITH threshold [log-rank, $P = 0.025$, HR = 0.47 (0.24–0.92)]; ITH threshold = 0 [log-rank, $P = 0.019$, HR = 0.21 (0.051–0.88)]; ITH threshold = 0.01 [log-rank, $P = 0.0096$, HR = 0.33 (0.14–0.79)]; and ITH threshold = 0.05 [log-rank, $P = 0.021$, HR = 0.45 (0.22–0.90)]. The number of patients in each group is listed below the survival curves.

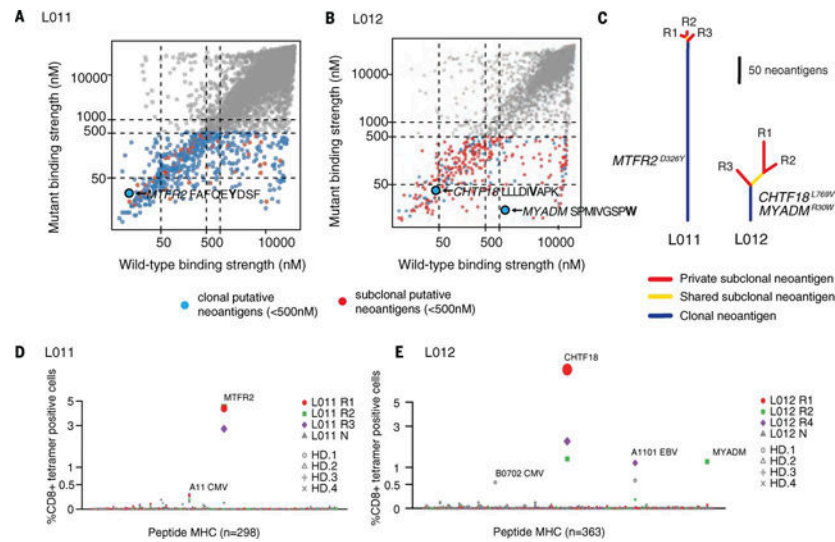


Fig. 2. Prediction and identification of neoantigen-reactive T cells in NSCLC samples
(A) Putative neoantigens predicted for all missense mutations in L011. The MTFR2^{D326Y} neoantigen (FAFQEYDSF) is highlighted. **(B)** Putative neoantigens predicted for all missense mutations in L012. The CHTF18^{L769V} neoantigen (LLLDIVAPK) and MYADM^{R30W} neoantigen (SPMIVGSPW) are indicated. **(C)** Evolutionary trees for L011 and L012 based on predicted neoantigens. **(D and E)** MHC-multimer screening of expanded, region-specific, tumor-infiltrating CD8⁺ T lymphocytes and healthy donor (HD) CD8⁺ PBMC controls with candidate neoantigens (L011, $n = 288$; L012, $n = 354$) and control HLA-matched viral peptides (L011, $n = 10$; L012, $n = 9$). Frequency of CD8⁺ MHC-multimer-positive cells out of total CD3⁺CD8⁺ tumor-infiltrating lymphocyte (TILs) is displayed for **(D)** and **(E)**, with size of symbol increasing with frequency.

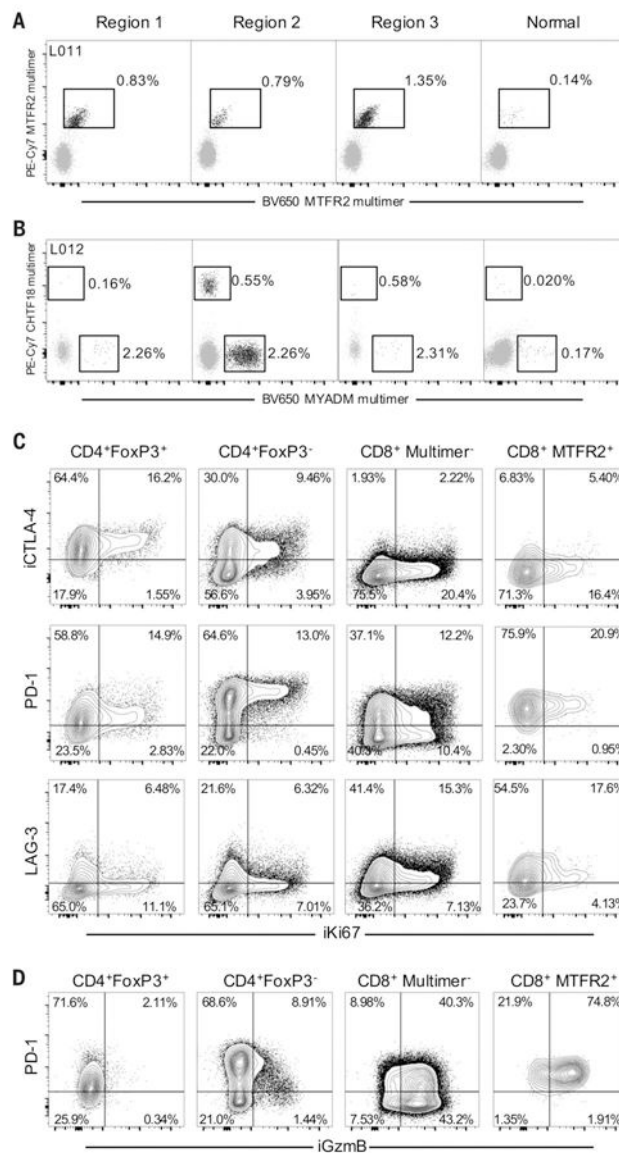


Fig. 3. Identification and characterization of tumor-infiltrating neoantigen-reactive CD8⁺ T cells in early-stage NSCLC

(A) MHC-multimer analysis of nonexpanded, tumor-infiltrating CD8⁺ T lymphocytes isolated from tumor regions 1 to 3 and normal lung tissue of patient L011 identifies CD8⁺ TILs reactive to mutant MTR2 peptide. (B) MHC-multimer analysis of nonexpanded, tumor-infiltrating CD8⁺ T lymphocytes isolated from tumor regions 1 to 3 and normal lung tissue of patient L012 identifies two distinct populations of CD8⁺ TILs reactive to mutant CHTF18 and MYADM peptide. The frequency of CD8⁺ MHC-multimer-positive cells out of total CD3⁺CD8⁺ TILs is displayed for (A) and (B). (C) Multiparametric flow cytometric analysis of tumor-infiltrating T lymphocyte subsets isolated from L011 region 3. Phenotypic data are representative of all tumor regions. Relative expression of iCTLA-4 (intracellular CTLA-4), surface PD-1, and surface LAG-3 by CD4⁺FoxP3⁺ (regulatory T cell), CD4⁺FoxP3⁻ (CD4 helper T cell), CD8⁺ multimer-negative, and CD8⁺ multimer-reactive (CD8⁺ MTR2⁺) T cells is displayed, plotted against iKi67 (intracellular Ki67). (D)

Coexpression of PD-1 and iGzmB (intracellular granzyme B) by tumor-infiltrating T lymphocyte subsets isolated from L011 region 3.

Author Manuscript

Author Manuscript

Author Manuscript

Author Manuscript

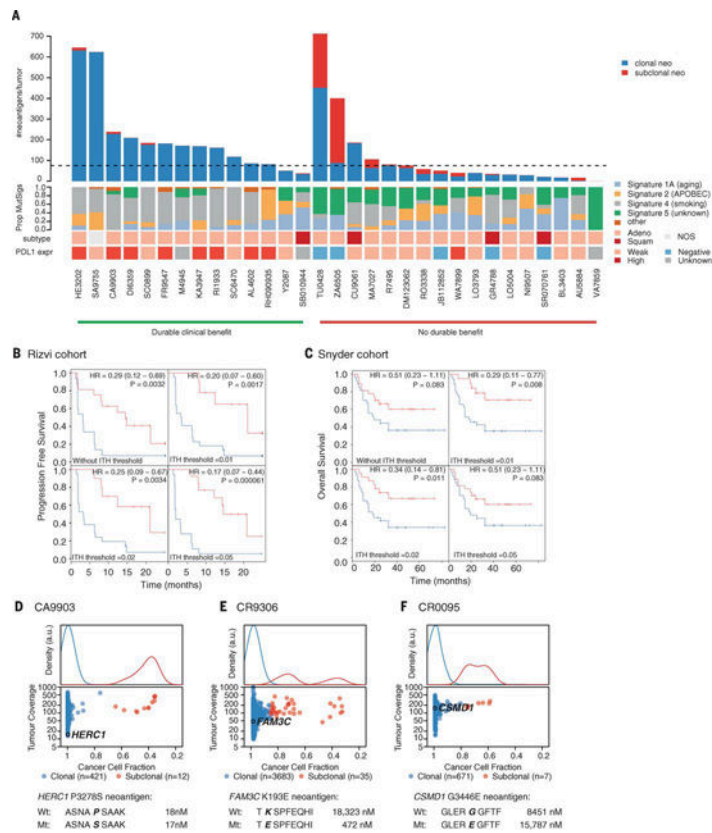


Fig. 4. Neoantigen clonal architecture and clinical benefit of immune checkpoint blockade
(A) Samples are grouped according to clinical benefit, with durable clinical benefit on left and no durable benefit on right [defined as in (2)]. Bar plot depicts clonal neoantigens in blue and subclonal neoantigens in red. Mutational signatures identified within each sample, subtype, and expression of PD-L1 are shown below. **(B)** Progression-free survival in NSCLC (2) cohort treated with antibody to PD1 either without an ITH threshold [HR = 0.29 (0.12–0.69), log-rank $P = 0.0032$] or with an ITH threshold of 0.01 [HR = 0.20 (0.07–0.60), log-rank $P = 0.0017$], 0.02 [HR = 0.25 (0.09–0.67), log-rank $P = 0.0034$], or 0.05 [HR = 0.17 (0.07–0.44), log-rank $P = 0.000061$]. **(C)** Overall survival in melanoma (4) cohort treated with antibody to CTLA-4 either without an ITH threshold [HR = 0.51 (0.23–1.11), $P = 0.083$] or with an ITH threshold of 0.01 [HR = 0.29 (0.11–0.77), log-rank $P = 0.008$], 0.02 [HR = 0.34 (0.14–0.81), log-rank $P = 0.011$], or 0.05 [HR = 0.51 (0.23–1.11), $P = 0.083$]. An ITH threshold of 0.05 results in the same survival curve as no ITH threshold because no tumors with a high neoantigen burden exhibit >0.05 neoantigen ITH. **(D to F)** Clonal architecture of (D) CA9903, (E) CR9306, and (F) CR0095, with mutations yielding neoantigens that elicit a Tcell response highlighted. Blue dots represent clonal mutations, with subclonal mutations depicted as red dots. Density plots are shown above.